TISSUE ENGINEERING: Part C
Volume 18, Number 9, 2012

DOI: 10.1089/ten.tec.2011.0621

Development of an Indirect Stereolithography Technology for Scaffold Fabrication with a Wide Range of Biomaterial Selectivity

Hyun-Wook Kang, Ph.D.,[1] and Dong-Woo Cho, Ph.D.[2,3]

Tissue engineering, which is the study of generating biological substitutes to restore or replace tissues or organs, has the potential to meet current needs for organ transplantation and medical interventions. Various approaches have been attempted to apply three-dimensional (3D) solid freeform fabrication technologies to tissue engineering for scaffold fabrication. Among these, the stereolithography (SL) technology not only has the highest resolution, but also offers quick fabrication. However, a lack of suitable biomaterials is a barrier to applying the SL technology to tissue engineering. In this study, an indirect SL method that combines the SL technology and a sacrificial molding process was developed to address this challenge. A sacrificial mold with an inverse porous shape was fabricated from an alkali-soluble photopolymer by the SL technology. A sacrificial molding process was then developed for scaffold construction using a variety of biomaterials. The results indicated a wide range of biomaterial selectivity and a high resolution. Achievable minimum pore and strut sizes were as large as 50 and 65 μm, respectively. This technology can also be used to fabricate three-dimensional organ shapes, and combined with traditional fabrication methods to construct a new type of scaffold with a dual-pore size. Cytotoxicity tests, as well as nuclear magnetic resonance and gel permeation chromatography analyses, showed that this technology has great potential for tissue engineering applications.

Introduction

Tissue engineering, the study of generating biological substitutes to restore or replace tissues or organs, has the potential to meet current needs for organ transplantation and medical interventions. Three key components of tissue engineering are the cells, cell signaling, and the scaffold. Recently, many researchers have applied solid freeform fabrication (SFF) for scaffold construction.[1–3] The SFF technology makes it possible to fabricate a porous structure with an arbitrarily designed inner and outer shape, and this design flexibility may help to overcome some of the difficulties in tissue engineering. Among the SFF technologies, stereolithography (SL) shows superior performance in the fabrication of three-dimensional (3D) structures.[4–13] The SL technology offers a fast fabrication speed and allows for high resolution. Above all, the SL technology based on multiphoton absorption showed the highest resolution of all 3D fabrication technologies.[4–6,10–13] Kawata *et al.*[4] reported fabrication of 3D structures with a sub-microscale resolution using the SL technology. Melissinaki *et al.*[10] introduced a high-resolution scaffold for neural tissue engineering with photocurable polylactide resin using the SL technology based on multiphoton absorption. Malinauskas *et al.*[11] reported fabrication of scaffolds with a several micrometer strut size for tissue engineering. The SL technology uses a photocuring process to construct 3D structures based on photopolymerization, so that photocurable biomaterial is essential point for tissue engineering applications using the SL technology. Although several photocurable biomaterials have been introduced for the SL technology,[10–16] many obstacles remain in applying these materials for medical interventions.

In the current study, an indirect SL technology was developed for the construction of scaffolds composed of clinically applicable biomaterials. This indirect SL method combines the SL technology and a sacrificial molding process. First, a sacrificial mold having an inverse porous shape was fabricated from an alkali-soluble photopolymer using the SL technology. We then designed and tested a new sacrificial molding process with a wide range of biomaterials, such as synthetic, natural, and nondegradable polymers. Dual-pore scaffolds[17] and 3D organ-shaped scaffolds based on a computer-aided design (CAD) model were also manufactured to demonstrate the usefulness of this technology. Finally, cytotoxicity tests as well as analysis with nuclear

[1]Wake Forest Institute for Regenerative Medicine, Winston-Salem, North Carolina.
[2]Department of Mechanical Engineering and [3]Division of Integrative Biosciences and Biotechnology, Pohang University of Science and Technology, Gyungbuk, South Korea.

magnetic resonance (NMR) and gel permeation chromatography (GPC) were conducted to assess the feasibility of this technology for tissue engineering applications.

Materials and Methods

The projection-based SL technology

A projection-based SL system, based on the technology first introduced by Bertsch *et al.*,[18] was built and applied to the fabrication of a sacrificial mold. Figure 1 shows a schematic drawing of the SL apparatus. It uses a 500W mercury ultraviolet (UV) lamp as a light source, a projection system based on a digital micromirror device (Texas Instruments, Inc.), and a three-axis stage system with 0.1 μm resolution/100 mm stroke. The projection system generates a 2D pattern image with microresolution. When an image is projected on the surface of a liquid photopolymer, a 2D pattern is generated by photopolymerization. A 3D structure can be constructed by stacking the 2D patterns.

Three-dimensional sacrificial mold

A mold structure having an inlet, outlet, and middle part was designed for injection molding process. The inlet was designed for direct connection to a syringe containing injectable biomaterial. The outlet was designed for removal of excess material and air. The middle of the mold was designed to have a porous shape for scaffold fabrication. With this design, the biomaterial-filling process can be conducted simply and without additional equipment. An alkali-soluble photopolymer introduced by Liska *et al.*[19] was used to construct a sacrificial mold. The preparation procedures were as follows: N,N-dimethyl-acrylamide (DMA), methacrylic acid (MA), and methacrylic anhydride (MAA) were carefully mixed by stirring at room temperature at a weight ratio of 40:40:7 (DMA:MA:MAA). Poly(vinyl pyrrolidone) (PVP; molecular weight: 360,000) powder of 13 wt% was then slowly added to the mixture, and additional stirring for 3–4 h was conducted to completely dissolve the PVP. Table 1 shows the final concentration of the mixture. The chemicals were purchased from Sigma-Aldrich. Finally, photoinitiator Irgacure 819 (Ciba Specialty Chemicals Co.) at 3 wt% was added to the solution with stirring for 3–4 h. Figure 2 shows an alkali-soluble photopolymer sacrificial mold fabricated using the projection-based SL technology.

Table 1. Alkali-Soluble Photopolymer Composition

N,N-Dimethyl-acrylamide	*Methacrylic acid*	*Methacrylic anhydride*	*Poly(vinyl pyrrolidone)*
40 wt%	40 wt%	7 wt%	13 wt%

Dissolution test using alkali-soluble photopolymer and various biomaterials

A dissolution test using NaOH solution was conducted for alkali-soluble photopolymer and biomaterials such as poly(DL-lactide-co-glycolide) (PLGA), polycaprolactone (PCL), poly(L-lactide) acid (PLLA), chitosan, alginate, and bone cement. Table 2 lists the biomaterials tested. For the dissolution test, samples of alkali-soluble photopolymer were prepared by UV curing on a glass plate. The other materials were used in their original form supplied by the manufacturer. First, the samples were dipped into a 1 N NaOH solution at 65°C and observed for 3 days. Then, a second experiment was conducted to investigate in detail the dissolution trends of PLGA and soluble photopolymer in various concentrations of NaOH at various temperatures. Samples of the PLGA and soluble polymer, $6.5 \times 6.5 \times 4.0\,mm^3$ in size, were prepared by casting using a Teflon mold at 90°C and the SL technology. The samples were immersed in various NaOH concentrations at various temperatures for predetermined duration. The samples were then washed with distilled water three times, freeze-dried, and finally weighed to determine the percentage of mass loss. The dissolution rate was calculated by curve-fitting the results using Excel.

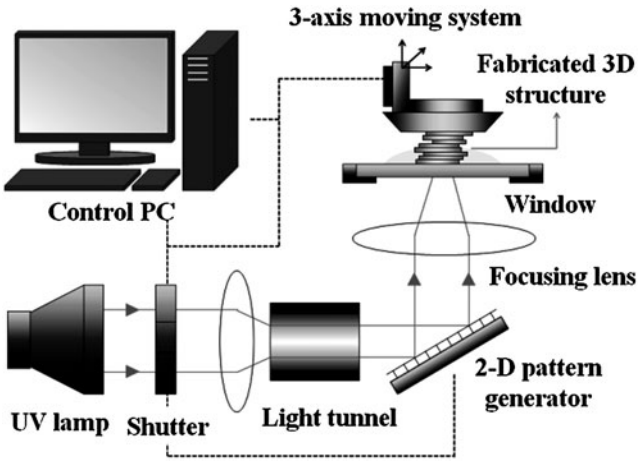

FIG. 1. Schematic drawing of the projection-based stereolithography (SL) system.

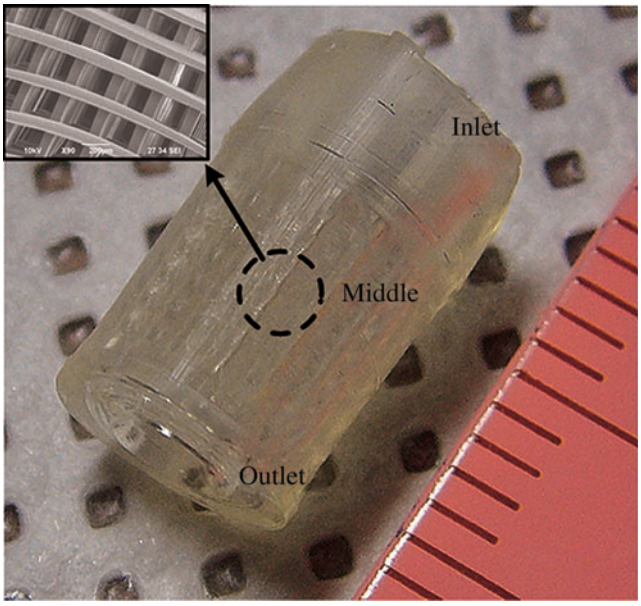

FIG. 2. Fabricated sacrificial porous mold composed of the alkali-soluble photopolymer. Color images available online at www.liebertonline.com/tec

Table 2. Biomaterials Applied for Scaffold Fabrication

Material	*Abbreviation*	*Source*
Polycaprolactone [$MW_{(weight\ avg)}$ = 65,000]	PCL	Sigma-Aldrich
Poly(DL-lactide-co-glycolide) (lactide:glycolide ratio, 65:35; MW = 40,000–75,000)	PLGA	
Chitosan (C3646, minimum 75% deacetylated)	—	
Sodium alginate powders (180947)	—	
Poly-L-lactide acid (PLLA, LX00111-158)	PLLA	Lakeshore Biomaterials (Brookwood Pharmaceuticals, Inc.)
Bone cement (EUROFIX GUN G)	—	Synergie Ingenierie Medicale, S.A.R.L.

Sacrificial molding processes using a wide range of biomaterials to construct unipore scaffolds

The general procedure for the sacrificial molding process is outlined in Figure 3. Injectable biomaterial was prepared using the appropriate solvent and was injected into the 3D porous mold fabricated by the SL technology. Next, the material was hardened by solvent/nonsolvent exchange or by cross-linking. The mold was then dissolved selectively in NaOH solution at a specific temperature by considering the results of the dissolution test. Table 3 lists the specific conditions used for the molding processes with various biomaterials. As shown in the table, about 6–45 h is required for hardening and mold removal after biomaterial injection. Final fabrication results were then obtained by air- or freeze-drying. Air-drying was conducted for synthetic polymers, whereas freeze-drying for 1 day was used for natural polymers. Each process was designed based on the properties of the biomaterial used.

Fabrication of dual-pore scaffolds by combining indirect SL and traditional methods

Phase inversion[20] and salt leaching,[21] which are two methods typically used for traditional scaffold fabrication, were combined with the proposed indirect SL technology to construct dual-pore scaffolds having designed global and local pores.[17] The fabrication procedures are described below.

Indirect SL combined with phase inversion. PCL grains were dissolved in N-N-dimethylacetamide (DMAc) at a ratio of 1:2 (w/w) by stirring the solution for 2 h at 50°C. After the solution was injected into the mold, it was cooled at room temperature for local pore generation by reducing the PCL solubility of DMAc.[20] The mold with PCL was then dipped into ethanol solution for 1 day to extract the DMAc. The mold was then removed using 1 N NaOH and the PCL scaffold was immersed in ethanol for 1 day to compete the extraction of DMAc. Finally, the mold was cleaned with distilled water and air-dried.

Indirect SL combined with salt leaching. PCL (20% w/v) solution was prepared with chloroform and mixed with salt sieves (100 μm mesh) at a salt:PCL ratio of 10:1 (w/w). The sacrificial mold was filled with the mixture using a syringe. After drying in a fume hood for 1 day to extract the chloroform, vacuum-drying was conducted to complete solvent removal. The sacrificial mold and salt were dissolved with 1 N NaOH and distilled water, respectively.

Complex 3D structure fabrication

The new indirect SL technology makes it possible to fabricate 3D freeform structures that imitate the shapes of human organs. To demonstrate this advantage, we applied the indirect SL technology to fabricate a scaffold having the

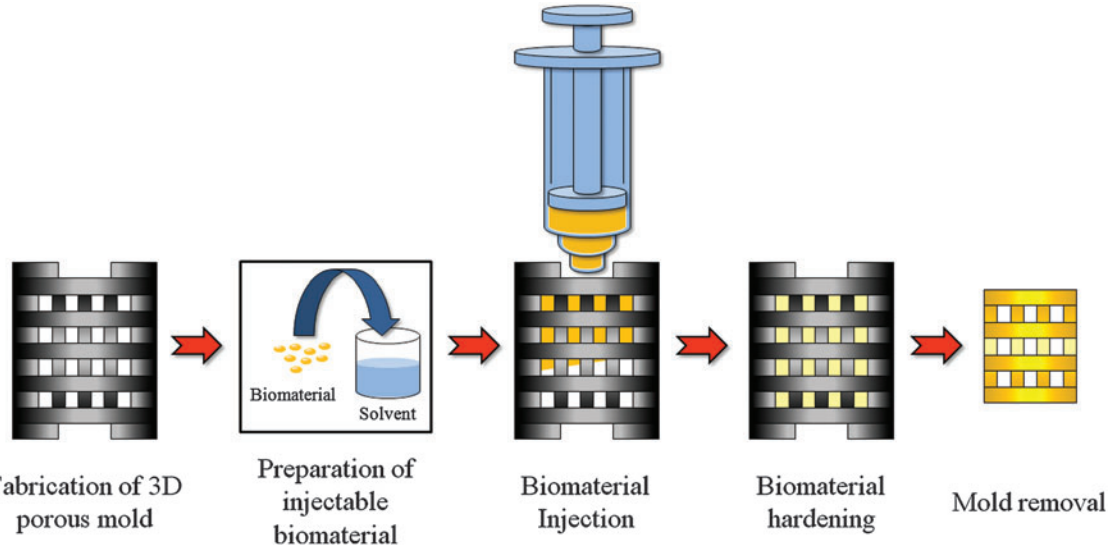

FIG. 3. Procedure of the indirect SL technology. 3D, three-dimensional. Color images available online at www.liebertonline.com/tec

Table 3. Molding Conditions Used for the Indirect Stereolithography Technology with Various Biomaterials to Construct Unipore Scaffolds

		Hardening process		*Mold removal*	
Material	*Preparation of injectable biomaterial*	*Method dipping process*	*Time (h)*	*NaOH (N)*	*Time (h)*
PCL	Chloroform/75% w/v	Solvent/nonsolvent exchange (isopropanol)	24	1	6
PLLA	Chloroform/25% w/v	Solvent/nonsolvent exchange (isopropanol)	12 (−80°C)/24	0.2	8 (0°C)
PLGA	Chloroform/75% w/v	Solvent/nonsolvent exchange (isopropanol)	12 (−80°C)/24	0.2	8 (0°C)
Chitosan	1 N Acetic acid/5% w/v	1 N NaOH	0.5	1	6
Alginate	Distilled water/6% w/v	5% w/v $CaCl_2$	3	1	6
Bone cement	Mixing powder and liquid	Self-hardening	0.1	1	6

Undefined process temperature is room temperature.

shape of a human tooth. A real human tooth was measured with microcomputed tomography (micro-CT), and the results were converted to the STL CAD format that is generally used in the SFF technology. A motion program was then obtained by applying the model to a CAD/CAM system made by us.[42] This motion program was transferred to the main computer and used to fabricate a sacrificial mold with an inverse shape using the SL technology. Finally, using PLGA with the molding process described above, a tooth-shaped scaffold was constructed.

Cytotoxicity test

The cytotoxicity of PLGA and PCL scaffolds was evaluated using a cell proliferation test. A total of 2×10^4 NIH3T3 cells were seeded into the 24-well plate and incubated overnight at 37°C. High-glucose Dulbecco's Modified Eagle Medium (DMEM) containing 10% v/v fetal bovine serum, 1% v/v penicillin, and 1% v/v antibiotics was used as the cell culture medium. After checking the morphology of seeded cells with a microscope, trans-well inserts containing cylindrical PLGA and PCL scaffolds of 4 mm diameter and 2 mm height were placed on the well plate. The normal cell group was cultured without any inserts on the well plate and used as a negative control. Latex inserts of 3 mm diameter were used as a positive control because of their cytotoxic effects.[22] The alamarBlue assay (Invitrogen, Inc.) was conducted to investigate cell proliferation of the plated cells on days 1, 3, 5, and 7. AlamarBlue (10% volume) was added to the cell culture medium and mixed well. Then, 500 μL of the solution was added to the 24-well plate after it was washed with PBS and incubated for 1 h at 37°C. The fluorescence intensity of 100 μL of the solution extracted from the plate was measured as recommended by the manufacturer. Cell viability was calculated by dividing the fluorescence intensity of samples by values of a normal cell culture group.

Measurements of mechanical properties

A cylindrical PLGA scaffold of 5 mm diameter and 2.5 mm height was prepared, and its mechanical properties were measured. The scaffold had a ~60% porosity and 200 μm strut size. The mechanical properties were tested using a universal testing machine (3344 model; Instron, Inc.), and the compressive modulus and strength were calculated from the stress–strain curve.

Analysis of fabrication results

Scanning electron microscopy (SEM), GPC, a microscope with vision system, and NMR were used to analyze the fabrication result of the scaffolds. The SEM and microscope were used for microstructure observations and measurements of their dimensions. To investigate the effect of the fabrication process on the properties of biomaterials, the molecular weight and composition of biomaterial before and after fabrication were measured by GPC and NMR, respectively. PLGA was applied for these measurements because its molecular weight is easily affected by fabrication process.[23–25]

Results

Dissolution test results of alkali-soluble photopolymer and biomaterials

Table 4 shows the results of the first dissolution test. The cured photopolymer and PLGA/PLLA were perfectly dissolved after 3–4 h and 1–2 days, respectively, at 65°C, whereas dissolution of PCL, alginate, chitosan, and bone cement did not occur even after 3 days.

Figure 4 shows the results of the second dissolution test using the photopolymer and PLGA. Fast dissolution of the photopolymer occurred for the first 2 hours, after which the mass loss was linear (Fig. 4A), whereas PLGA exhibited a linear dissolution rate throughout (Fig. 4B). High concentration

Table 4. Dissolution in 1 N NaOH Solution at 65°C for 3 Days

Material	*Dissolution time*
Alkali-soluble photopolymer	3–4 h
PLGA	1–2 days
PLLA	
PCL	Insoluble
Alginate	
Chitosan	
Bone cement	

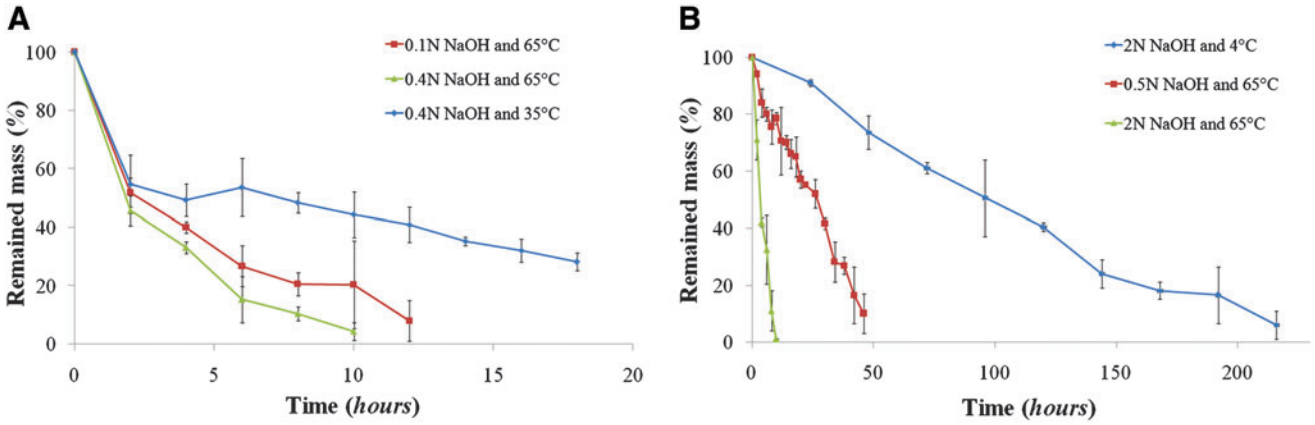

FIG. 4. Dissolution test results of cured alkali-soluble photopolymer **(A)** and poly(DL-lactide-co-glycolide) (PLGA) **(B)** at various NaOH concentrations and temperatures ($n=3$). Color images available online at www.liebertonline.com/tec

Table 5. Dissolution Rate of Poly(DL-Lactide-Co-Glycolide) and Alkali-Soluble Photopolymer in NaOH Solution

	Akali-soluble photopolymer		*PLGA*	
NaOH concentration (N)	*4°C*	*65°C*	*4°C*	*65°C*
0.1	—	4.053 ($R^2=0.778$)	—	
0.4	1.726 ($R^2=0.720$)	5.267 ($R^2=0.872$)		
0.5	—		—	1.842 ($R^2=0.957$)
2			0.446 ($R^2=0.953$)	9.778 ($R^2=0.943$)

Dissolution rate means mass loss % per hour.

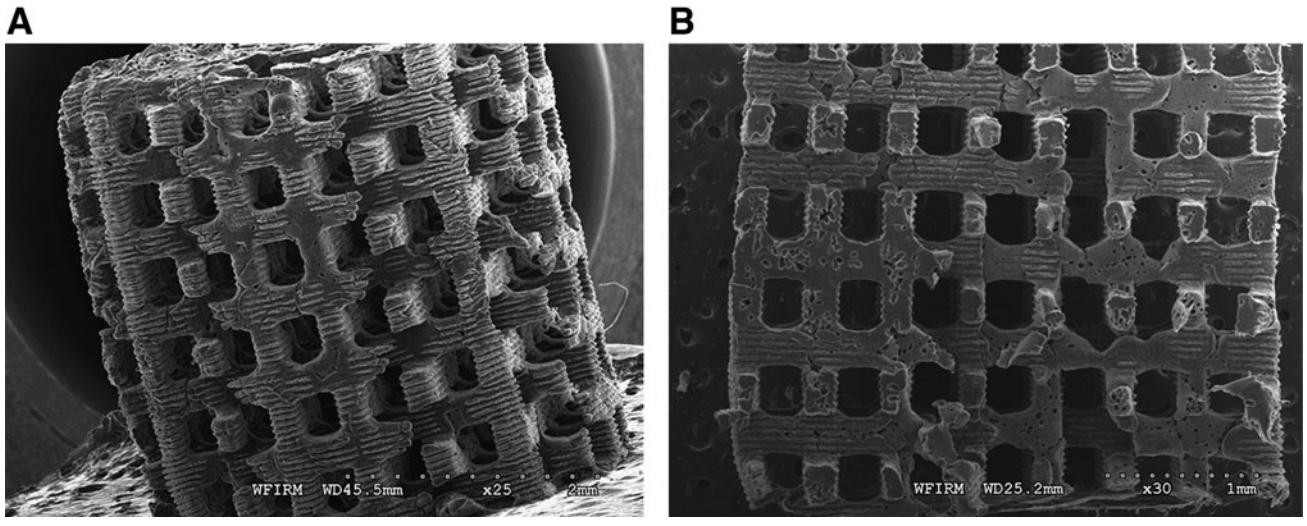

FIG. 5. Scanning electron microscope images of a fabricated polycaprolactone (PCL) scaffold **(A)** and its cut end **(B)**.

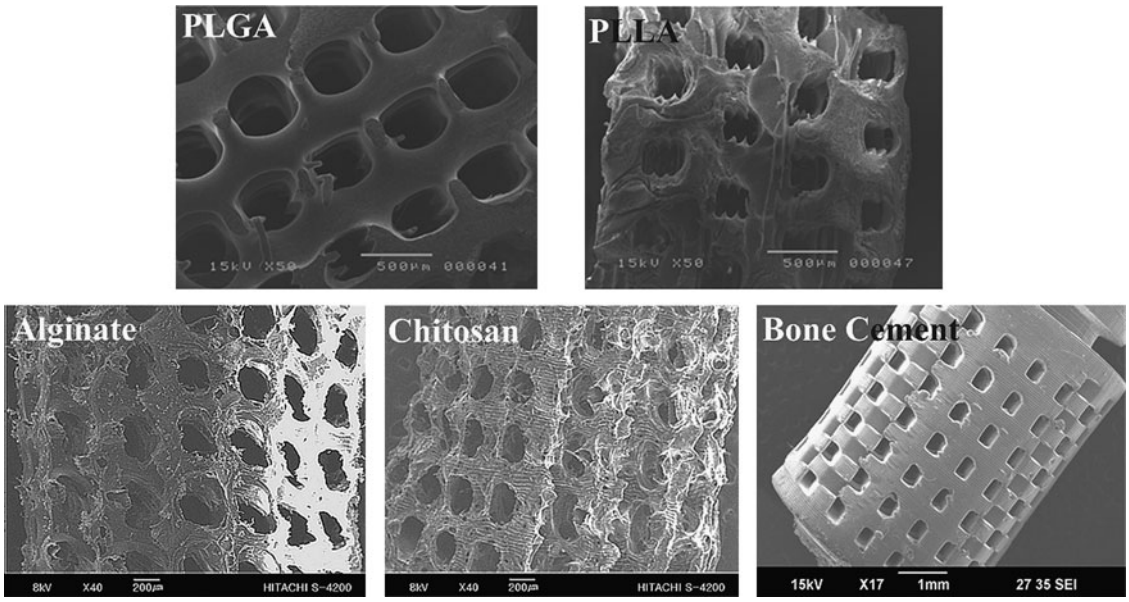

FIG. 6. Three-dimensional porous scaffolds with pore sizes of 200–400 μm fabricated using PLGA, poly(L-lactide) acid (PLLA), alginate, chitosan, and bone cement as biomaterials.

of NaOH and high temperature accelerated the dissolution rates of PLGA and soluble photopolymer. The rate of mass loss was calculated by linear curve fitting based on these results; in the case of soluble photopolymer, only the data after the first 2 hours were used. As shown in Table 5, a reduction of NaOH concentration to 25% of the initial value at 65°C resulted in about 23% decrease of dissolution rate for the soluble photopolymer and about 81% decrease for PLGA. A reduction of the temperature from 65°C to 4°C resulted in about 67% decrease in the dissolution rate for the photopolymer and about 95% decrease for PLGA. These reduction percentages were calculated using 0.4 N concentration for the alkali-soluble photopolymer and 2 N for PLGA at 65°C. PLGA experienced a greater reduction of dissolution rate than the soluble photopolymer as the NaOH concentration and temperature decreased, and this difference increased as the NaOH concentration and temperature decreased further. This is important in developing the mold removal process for fabricating PLGA and PLLA scaffolds.

Three-dimensional porous scaffolds

Various fabrication results were obtained using the described procedures with each biomaterial (Table 3). Figure 5 shows the fabricated PCL scaffold and its cut-end image. As shown in Figure 5A, a well-constructed pore architecture of rectangular shape was observed, with a pore size of ~300 μm and a 200-μm strut size. Several defect structures were observed in the cross-section view (Fig. 5B), which were caused by entrapped bubbles in the injection process. However, overall pore architecture was well constructed and no mold structure was detected. Figure 6 shows SEM images of fabricated structures composed of other biomaterials. A 3D porous scaffold with rectangular pores of 200–400 μm was well fabricated using synthetic polymers (PLGA and PLLA), natural polymers (chitosan and alginate), and non-degradable biomaterial (bone cement) (Fig. 6). The achievable minimum pore and strut sizes were about 50 and 65 μm, respectively, using the proposed method (Fig. 7).

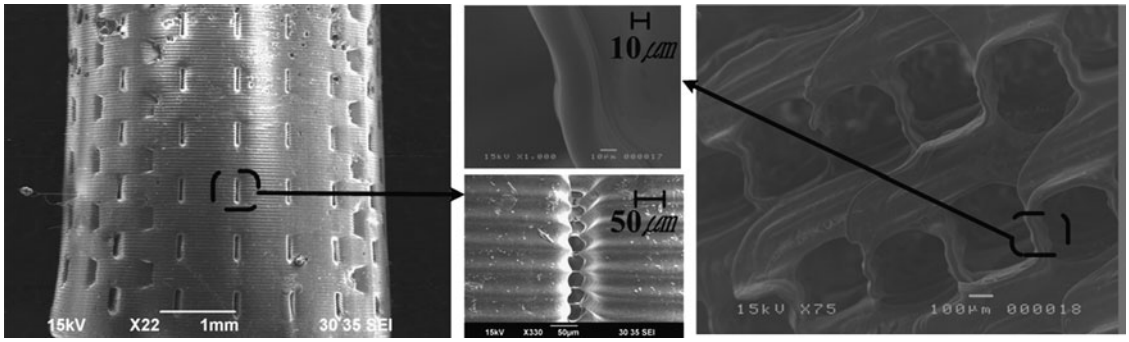

FIG. 7. Fabricated 3D porous scaffolds of about 50 μm pore size (bone cement, left figure) and 65 μm strut size (PLGA, right figure).

Table 6. Mechanical Properties of the Poly(DL-Lactide-Co-Glycolide) Scaffold (N = 3)

Compressive strength	*Compressive modulus*
1.08 ± 0.324 MPa	20.1 ± 5.63 MPa

Table 6 shows the measured mechanical properties of PLGA scaffolds fabricated using the indirect SL technology. Such scaffolds exhibited a compressive strength and modulus of ~1.08 and 20.1 MPa, respectively. Kim *et al.*[26] reported similar results (compressive strength and modulus of 1 and 17.8 MPa, respectively) for a PLGA scaffold with a 50% porosity, 200 μm strut size, and a molecular weight of 50,000–75,000. Our scaffold exhibited a ~60% porosity, 200 μm strut size, and molecular weight of 40,000–75,000. Although the two results cannot be directly compared, they suggest that the indirect SL technology did not result in a significant change in the mechanical properties of PLGA.

Figure 8 shows the fabricated dual-pore scaffolds. The structures contained large pores measuring 300–400 μm and small pores measuring either 1–5 μm when created by phase inversion (Fig. 8A) or 30–100 μm when created by salt leaching (Fig. 8B). The inner architecture composed of large pores can be controlled by changing the mold design.

Figure 9 illustrates the fabrication of the human-tooth-shaped scaffold. From a 3D CAD model generated based on 3D micro-CT measurements of a real tooth, a porous mold having the inverse tooth shape was constructed by the SL system. The sacrificial molding process was applied using PLGA for scaffold fabrication. A 3D tooth-shaped scaffold containing microscale rectangular pores was constructed successfully.

Cytotoxicity test results

Figure 10 shows results of cell viability tests measured using the alamarBlue assay. The cell viability of PLGA and PCL scaffolds fabricated by the indirect SL technology was more than 90% for 7 days, compared to only less than 10% for the latex sample. This indicates that the scaffold fabricated with the indirect SL technology did not have any cytotoxic effect on cell proliferation.

NMR and GPC results

Figure 11 displays the NMR spectra of PLGA raw material, alkali-soluble photopolymer, and PLGA scaffold material, respectively. A comparison among the three spectra showed that no alkali-soluble photopolymer remained in the fabricated PLGA scaffold. Figure 12 shows GPC measurement results. Based on the GPC results for the PLGA raw and scaffold materials, the molding process did not significantly affect the molecular weight of PLGA.

Discussion

To date, various SFF-based indirect methods of scaffold fabrication and tissue engineering applications of these methods have been reported.[17,27–32] Sachlos *et al.*[27,28] introduced a collagen scaffold fabricated by an indirect method using an ink-jet printer. Moreover, Taboas *et al.*[17] investigated an indirect construction method of dual-pore/composite scaffolds. In contrast, although the SL technology has many advantages in terms of fabrication speed and resolution, the indirect methods based on the SL technology reported thus far have used agarose, silicone, and ceramic powders.[19,33,34]

In this research, the indirect SL technology was studied for the production of scaffolds with various biomaterials, such as PLGA, PLLA, PCL, chitosan, alginate, and bone cement, which are generally used in tissue engineering. The process for the indirect SL technology consists of three steps: fabrication of the sacrificial mold, injection molding, and selective removal of the mold. First, this research has demonstrated the processability of alkali-soluble photopolymer through the fabrication of 3D porous molds using the SL technology (Fig. 2). The molding process required no equipment other than a syringe because the mold had both an inlet and an outlet. Second, the sacrificial molding processes were designed to take into account the intrinsic physical and chemical properties of each biomaterial. Chloroform, acetic acid, and distilled water were used to produce injectable material. After injection molding, solvent/nonsolvent exchange was used to extract organic solvent from the injected PLGA, PCL, and PLLA solutions. Chitosan and alginate gel formation was obtained using NaOH and $CaCl_2$ solutions, respectively. Third, selective removal of the mold, the last and most important process, must not result in any defects in the biomaterial structure in the mold. In this research, dissolution tests were conducted for alkali-soluble photopolymer and the other biomaterials. The cured alkali-soluble photopolymer was perfectly dissolved after 3–4 h at 65°C (Table 4), whereas significant dissolution of PCL, alginate, chitosan, and bone cement did not occur even after 3 days (Table 4). On the other hand, PLGA and PLLA dissolved in 1–2 days in

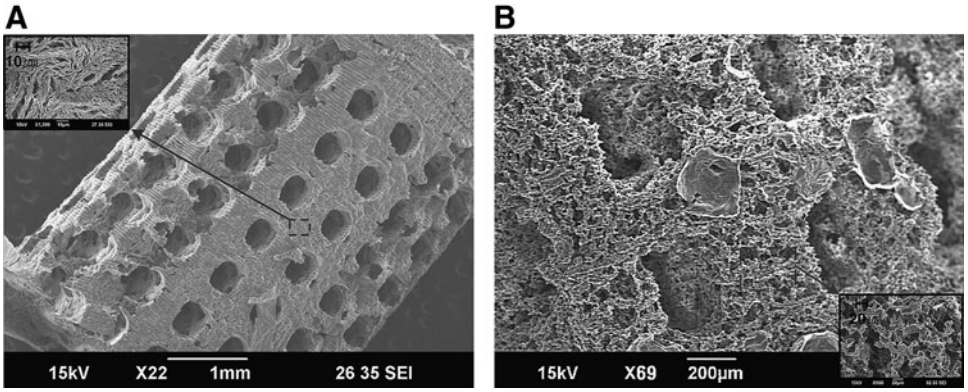

FIG. 8. Fabricated 3D dual-pore scaffolds constructed of PCL using a molding process combined with phase inversion **(A)** or salt leaching **(B)**.

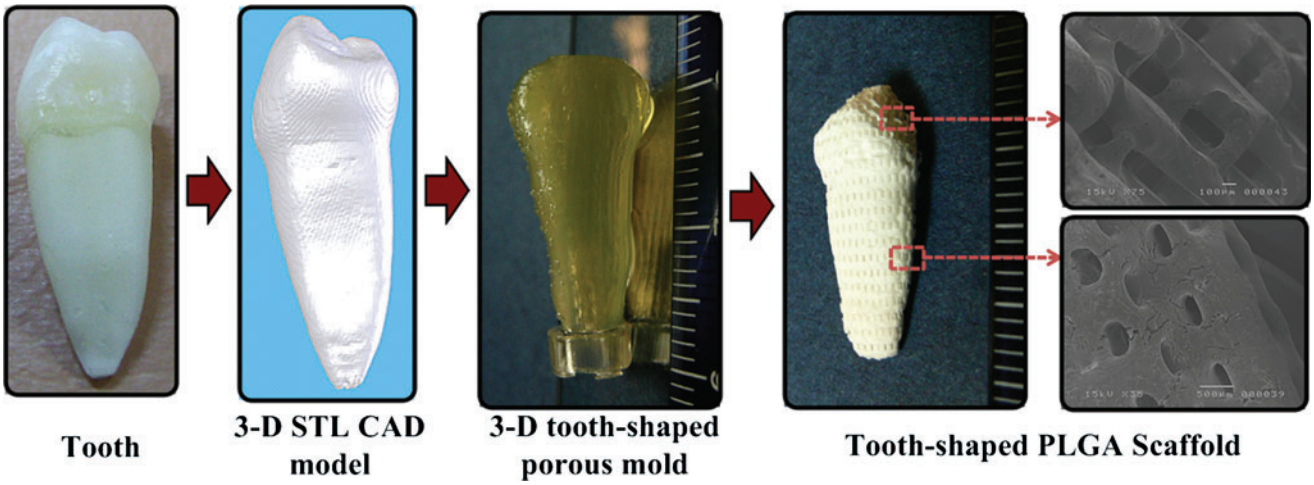

FIG. 9. Fabrication of a tooth-shaped PLGA scaffold. Color images available online at www.liebertonline.com/tec

the NaOH solution. The accelerated dissolution of PLGA and PLLA is related to the pH level of the NaOH solution. Burkersroda *et al.*[35] examined the degradation mechanisms of PLGA and PLLA at various pH levels. They showed that surface erosion was generated in NaOH solutions of high pH, but the material properties were unaffected. In addition, many researchers have investigated the use of surface treatment with NaOH solutions of high pH to enhance the cell affinity of scaffolds composed of synthetic polymers such as PLGA, PCL, and PLLA.[36–41] Various properties were measured, such as molecular weight, glass transition temperature, melting temperature, enthalpy of melting, and atomic components. NaOH treatment did not significantly affect these properties.[36–38] Our data regarding GPC and mechanical properties of PLGA scaffolds fabricated by the indirect SL technology showed a similar trend. No significant changes in biomaterial properties were observed.

An experiment was conducted to investigate dissolution trends of alkali-soluble photopolymer and PLGA. The results showed that the difference in the dissolution rates of these two materials can be maximized by reducing both the concentration of NaOH and the temperature. This result is significant for minimizing structural defects due to high pH in the mold removal process; 0.2 N NaOH at 0°C was used for the mold removal process in PLGA and PLLA scaffold fabrication. This work has led to a well-designed molding process and successful fabrication of scaffolds using PLGA, PLLA, PCL, chitosan, alginate, and bone cement. The technology has a wide range of biomaterial selectivity and high resolution. Various factors affect fabrication resolution. The highest achievable mold resolution using the SL technology was ~50–70 μm. Furthermore, the achieved minimum pore size and strut size were also 50 and 65 μm, respectively (Fig. 7). The properties of biomaterials used in the molding process also affect the fabrication results. Synthetic polymers showed results comparable with mold dimensions. In contrast, an isotropic shrinkage of 40%–60% was observed during fabrication of scaffolds with natural polymers, which occurred during freeze-drying.

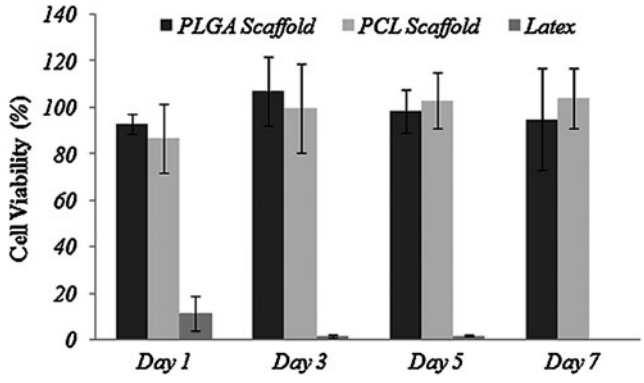

FIG. 10. Cytoxocity test results ($n = 5$).

This technology can also be combined with traditional technologies, such as salt leaching and phase inversion, to fabricate dual-pore scaffolds.[17] The size of the large pores in the inner architecture of the dual-pore scaffold can be controlled to optimize the mechanical strength as well as the fluid dynamics for nutrient and oxygen supplies to seeded cells. Based on micro-CT measurement results, the fabrication of a 3D tooth-shaped scaffold demonstrated that this technology can be applied to the construction of scaffolds with a 3D organ shape.

The results of cytotoxicity testing, NMR, and GPC showed that the scaffolds fabricated with the indirect SL technology are quite suitable for tissue engineering applications. NMR results and cytotoxicity measurements showed that the scaffolds did not have any mold residue and generate any cytotoxic effect. GPC results indicated that the fabrication procedures did not significantly affect the molecular weight of the biomaterial.

Compared with other SFF methods,[1–3] the indirect method presented here requires an additional molding process. However, it offers notable advantages in material selectivity, as a wide range of biomaterials can be applied to this technology. Sophisticated adjustment of biomaterial composition is central to achieving proper degradability and physical strength.[1] The indirect SL technology developed in the current study makes it possible to fabricate a 3D structure composed of well-designed biomaterials. Above all, this technology has much potential for improving the fabrication

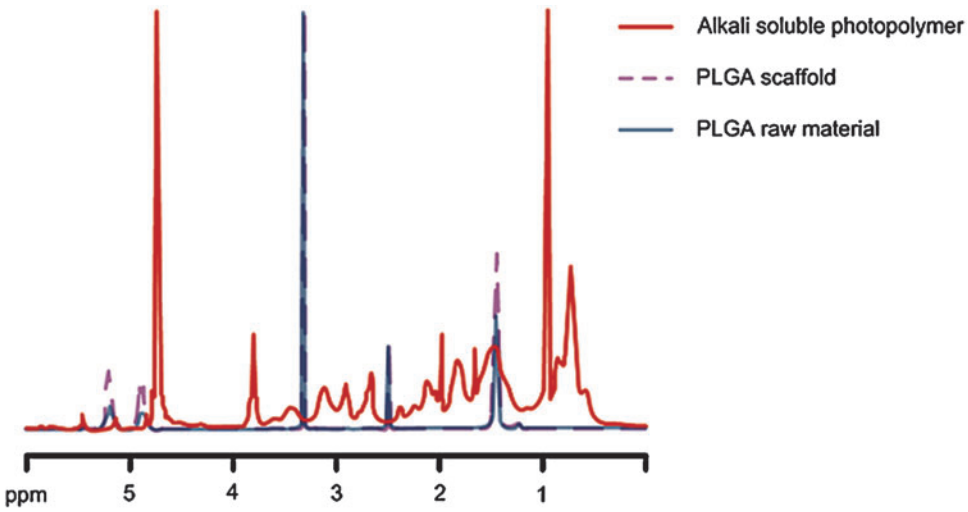

FIG. 11. Nuclear magnetic resonance spectra of PLGA raw material, PLGA scaffold, and alkali-soluble photopolymer. Color images available online at www.liebertonline.com/tec

resolution. Among various 3D fabrication technologies, the SL technology not only shows the highest resolution but also offers fast fabrication speed.[4–13] The reported highest resolution was nanoscale in 3D space. We will continue to examine methods for fabricating high-resolution molds and molding processes on a nano/micrometer scale using various biomaterials. Further development of this technology will provide a new paradigm for the construction of 3D structures composed of biomaterials.

Conclusion

In this research, the indirect SL technology was developed for fabrication of 3D organ-shaped scaffolds using a wide range of biomaterials. In the process, 3D porous molds were constructed of alkali-soluble photopolymer, and sacrificial molding processes were sophisticatedly designed and realized by considering the properties of the biomaterials. Using these procedures, the achievable minimum pore and strut sizes were on a scale of several tens of micrometers, and the application of a large selection of biomaterials, including PCL, PLGA, PLLA, chitosan, alginate, and bone cement, for scaffold fabrications was demonstrated. In addition, dual-pore scaffolds were successfully fabricated by combining indirect SL with phase inversion or salt leaching. Cytotoxicity, NMR, and GPC results confirmed that the technology can be safely applied to the fabrication of products for tissue engineering and medical interventions. Collectively, the current findings illustrate the successful development of the new indirect SL technology capable of providing excellent performance with a large selection of biomaterials.

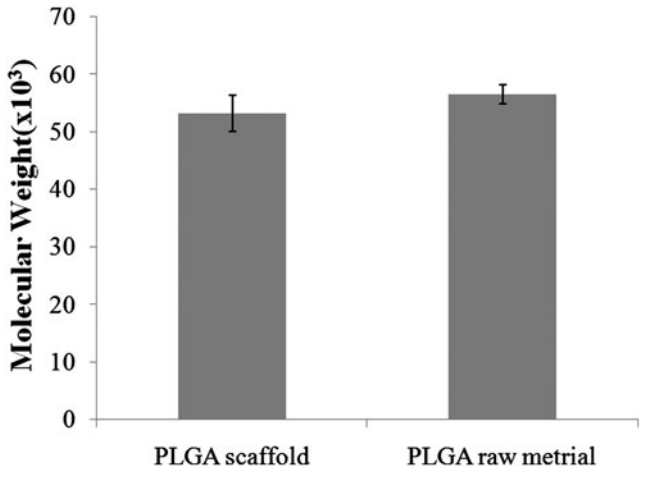

FIG. 12. Gel permeation chromatography measurement of PLGA raw and scaffold material ($n = 3$).

Acknowledgment

This work was supported by the National Research Foundation of Korea (NRF) grant funded by the Korea government (MEST; no. 2011-0000412).

Disclosure Statement

No competing financial interests exist.

References

1. Yeong, W.-Y., Chua, C.-K., Leong, K.-F., and Chandrasekaran, M. Rapid prototyping in tissue engineering: challenges and potential. Trends Biotechnol **22,** 643, 2004.
2. Hutmacher, D.W., Sittinger, M., and Risbud, M.V. Scaffold-based tissue engineering: rationale for CAD and SFF systems. Trends Biotechnol **22,** 354, 2004.
3. Lee, J.W., Cuddihy, M.J., and Kotov, N.A. Three-dimensional cell culture matrices: state of the art. Tissue Eng Part B **41,** 61, 2008.
4. Kawata, S., Sun, H.-B., Tanaka, T., and Takada, K. Finer features for functional microdevices. Nature **412,** 697, 2001.
5. Lee, S.-H., Moon, J.J., and West, J.L. Three-dimensional micropatterning of bioactive hydrogels via two-photon laser scanning photolithography for guided 3D cell migration. Biomaterials **29,** 2962, 2008.
6. Yang, D.-Y., Lim, T.W., Son, Y., Kong, H.-J., Lee, K.-S., Kim, D.-P., and Park, S.H. Additive process using femto-second laser for manufacturing three-dimensional nano/microstructures. Int J Precision Eng Manuf **8,** 63, 2007.
7. Ikuta, K., and Maruo, S. Submicron stereolithography for the production of freely movable mechanisms by using single-photon polymerization. Sens Actuators A Phys **100,** 70, 2002.

8. Sun, C., Fang, N., Wu, D.M., and Zhang, X. Projection micro-stereolithography using digital micro-mirror dynamic mask. Sens Actuators A Phys **121,** 113, 2005.
9. Kang, H.-W., Lee, I.H., and Cho, D.-W. Development of an assembly-free process based on virtual environment for fabricating 3D microfluidic systems using microstereolithography technology. Trans ASME J Manuf Sci Eng **126,** 766, 2004.
10. Melissinaki, V., Gill, A.A., Ortega, I., Vamvakaki, M., Ranella, A., Haycock, J.W., Fotakis, C., Farsari, M., and Claeyssens, F. Direct laser writing of 3D scaffolds for neural tissue engineering applications. Biofabrication **3,** 045005, 2011.
11. Malinauskas, M., Danilevičius, P., Baltriukienė, D., Rutkauskas, M., Žukauskas, A., Kairytė, Ž., Bičkauskaitė, G., Purlys, V., Paipulas, D., Bukelskienė, V., and Gadonas, R. 3D artificial plymeric scaffolds for stem cell growth fabricated by femtosecond laser. Lithuanian J Phys **50,** 75, 2010.
12. Engelhardt, S., Hoch, E., Borchers, K., Meyer, W., Kruger, H., Tovar, G., and Gillner, A. Fabrication of 2D protein microstructures and 3D polymer–protein hybrid microstructures by two-photon polymerization. Biofabrication **3,** 025003 3, 2011.
13. Lee, S.-J., Kang, H.-W., Park, J.K., Rhie, J.-W., Hahn, S.K., and Cho, D.-W. Application of microstereolithography in the development of three-dimensional cartilage regeneration scaffolds. Biomed Microdevices **10,** 233, 2008.
14. Lee, J.W., Lan, P.X., Kim, B., Lim, G.B., and Cho, D.-W. 3D scaffold fabrication with PPF/DEF using micro-stereolithography. Microelectron Eng **84,** 1702, 2007.
15. Kwon, I.K., and Matsuda, T. Photo-polymerized micro-architectural constructs prepared by microstereolithography (muSL) using liquid acrylate-end-capped trimethylene carbonate-based prepolymers. Biomaterials **26,** 1675, 2005.
16. Cooke, M.N., Fisher, J.P., Dean, D., Rimnac, C., and Mikos, A.G. Use of stereolithography to manufacture critical-sized 3D biodegradable scaffolds for bone ingrowth. J Biomed Mater Res **64B,** 65, 2002.
17. Taboas, J.M., Maddox, R.D., Krebsbach, P.H., and Hollister, S.J. Indirect solid free form fabrication of local and global porous, biomimetic and composite 3D polymer-ceramic scaffolds. Biomaterials **24,** 181, 2003.
18. Bertsch A., Zissi S., Jézéquel J.Y., Corbel S., and André J.C. Microstereophotolithography using a liquid crystal display as dynamic mask-generator. Microsyst Technol **3,** 42, 1997.
19. Liska, R., Schwager, F., Maier, C., Cano-Vives, R., and Stampfl, J. Water-soluble photopolymers for rapid prototyping of cellular materials. J Appl Polym Sci **97,** 2286, 2005.
20. Causa, F., Netti, P.A., Ambrosio, L., Ciapetti, G., Baldini, N., Pagani, S., Martini, D., and Giunti, A. Poly-ε-caprolactone/hydroxyapatite composites for bone regeneration: *in vitro* characterization and human osteoblast response. J Biomed Mater Res A **76A,** 151, 2006.
21. Kang, K.S., Lee, S.-J., Lee, H., Moon, W., and Cho, D.-W. Effects of combined mechanical stimulation on the proliferation and differentiation of pre-osteoblasts. Exp Mol Med **43,** 367, 2011.
22. Hanson, M., and Lobner D. *In vitro* neuronal cytotoxity of latex and nonlatex orthodontic elastics. Am J Orthod Dentofacial Orthop **126,** 65, 2004.
23. Kikuchi, M., Suetsugu, Y., Tanaka, J., and Akao, M. Preparation and mechanical properties of calcium phosphate/copoly-L-lactide composites. J Mater Sci Mater Med **8,** 361, 1997.
24. Rothen-Weinhold, A., Besseghir, K., Vuaridel, E., Sublet, E., Oudry, N., Kubel, F., and Gurny, R. Injection-molding versus extrusion as manufacturing technique for the preparation of biodegradable implants. Eur J Pharm Biopharm **48,** 113, 1999.
25. Shim, J.-H., Kim, J.Y., Park, J.K., Hahn, S.K., Rhie, J.-W., Kang, S.-W., Lee, S.-H., and Cho, D.-W. Effect of thermal degradation of SFF-based PLGA scaffolds fabricated using a multi-head deposition system followed by change of cell growth rate. J Biomater Sci Polym Ed **21,** 1069, 2010.
26. Kim, J.Y., Park, E.K., Kim, S.-Y., Shin, J.-W., and Cho, D.-W. Fabrication of a SFF-based three-dimensional scaffold using a precision deposition system in tissue engineering. J Micromech Microeng **18,** 055027, 2008.
27. Sachlos, E., Reis, N., Ainsley, C., Derby B., and Czernuszka, J.T. Novel collagen scaffolds with predefined internal morphology made by solid freeform fabrication. Biomaterials **24,** 1487, 2003.
28. Sachlos, E., Wahl, D.A., Triffitt, J.T., and Czernuszka, J.T. The impact of critical point drying with liquid carbon dioxide on collagen-hydroxyapatite composite scaffolds. Acta Biomater **4,** 1322, 2008.
29. Taylor, P.M., Sachlos, E., Dreger, S.A., Chester, A.H., Czernuszka, J.T., and Yacoub, M.H. Interaction of human valve interstitial cells with collagen matrices manufactured using rapid prototyping. Biomaterials **27,** 2733, 2006.
30. Lee, M., Dunn, J.C.Y., and Wu, B.M. Scaffold fabrication by indirect three-dimensional printing. Biomaterials **26,** 4281, 2005.
31. Mondrinos, M.J., Dembzynski, R., Lu, L., Byrapogu, V.K., Wootton, D.M., Lelkes, P.I., and Zhou, J. Porogen-based solid freeform fabrication of polycaprolactone-calcium phosphate scaffolds for tissue engineering. Biomaterials **27,** 4399, 2006.
32. Hollister, S.J., Maddox, R.D., and Taboas, J.M. Optimal design and fabrication of scaffolds to mimic tissue properties and satisfy biological constraints. Biomaterials **23,** 4095, 2002.
33. Sanchez-salcedo, S., Nieto, A., and Vallet-regi, M. Hydroxyapatite/β-tricalcium phosphate/agarose macroporous scaffolds for bone tissue engineering. Chem Eng J **137,** 62, 2008.
34. Gabriel Chu, T.-M., Orton, D.G., Hollister, S.J., Feinberg, S.E., and Halloran, J.W. Mechanical and *in vivo* performance of hydroxyapatite implants with controlled architectures. Biomaterials **23,** 1283, 2002.
35. Burkersroda, F., Schedl, L., and Gopferich, A. Why degradable polymers undergo surface erosion or bulk erosion. Biomaterials **23,** 4221, 2002.
36. Croll, T.I., O'Connor, A.J., Stevens, G.W., and Cooper-White, J.J. Controllable surface modification of poly(lactic-co-glycolic acid) (PLGA) by hydrolysis or aminolysis I: physical, chemical, and theoretical aspects. Biomacromolecules **5,** 463, 2004.
37. Gao, J., Niklason, L., and Langer, R. Surface hydrolysis of poly(glycolic acid) meshes increases the seeding density of vascular smooth muscle cells. J Biomed Mater Res **42,** 417, 1998.
38. Thapa, A., Miller, D.C., Webster, T.J., and Haberstroh, K.M. Nano-structured polymers enhance bladder smooth muscle cell function. Biomaterials **24,** 2915, 2003.
39. Pattison, M.A., Wurster, S., Webster, T.J., and Haberstroh, K.M. Three-dimensional, nano-structured PLGA scaffolds for bladder tissue replacement applications. Biomaterials **26,** 2491, 2005.

40. Kay, S., Thapa, A., Haberstroh, K.M., and Webster, T.J. Nanostructured polymer/nanophase ceramic composites enhance osteoblast and chondrocyte adhesion. Tissue Eng **8,** 753, 2002.
41. Smith, L.L., Niziolek, P.J., Haberstroh, K.M., Nauman, E.A., and Webster, T.J. Decreased fibroblast and increased osteoblast adhesion on nanostructured NaOH-etched PLGA scaffolds. Int J Nanomed **2,** 383, 2007.
42. Jung, J.W., Kang, H.-W., Kang, T.-Y., Park, J.H., Park, J., and Cho, D.-W. Projection Image-generation algorithm for fabrication of a complex structure using projection-based microstereolithography. International Journal of Precision Engineering and Manufacturing **13,** 445, 2012.

Address correspondence to:
Dong-Woo Cho, Ph.D.
Department of Mechanical Engineering
Pohang University of Science and Technology
San 31, Hyoja dong, Nam-gu, Pohang
Gyungbuk 790-784
South Korea

E-mail: dwcho@postech.ac.kr

Received: November 2, 2011
Accepted: March 21, 2012
Online Publication Date: April 27, 2012